Calculation of Planar and Conical Diffuser Flows

Y. G. Lai* and R. M. C. So†
Arizona State University, Tempe, Arizona
and
B. C. Hwang‡
Naval Ship Research and Development Center, Annapolis, Maryland

A numerical investigation of the near-wall turbulent flow in a planar and a conical diffuser is presented. The numerical calculation is based on the fully conserved control volume representation of the governing equations and the closure of the governing equations is achieved by a modified version of a low Reynolds number k-ϵ model, which takes into account the severe adverse pressure gradient effects encountered in diffuser flows. At zero pressure gradient, the modified near-wall turbulence model asymptotes correctly to the original model developed by Chien, which is successful in predicting simple turbulent shear flows. The calculated results are compared with measurements in a planar diffuser having a divergence angle of approximately 1 deg and in a conical diffuser having a total divergence angle of 8 deg. Good agreement is obtained for both diffuser flows. Furthermore, comparisons are made of the present results with those obtained by invoking the wall-function approximations and those given by Chien's low Reynolds number k-ϵ model. The inadequacy of the wall-function approximations and the need to correct for pressure gradient effects are clearly demonstrated.

Nomenclature

C_p = wall static pressure coefficient
$(C_p)_{\min}$ = minimum wall static pressure coefficient
C_3, C_4, C_5 = model constants
$C_{\epsilon 1}, C_{\epsilon 2}, C_\mu$ = model constants
f_1, f_μ = near-wall model functions
G = production of turbulence energy
k = turbulent kinetic energy
p = mean static pressure
p^+ = dimensionless pressure gradient parameter, $= (\mu/\rho^2 u_\tau^3)(\partial p/\partial r)_{\text{wall}}$
r = radial coordinate
Re = inlet Reynolds number, $= U_{\text{in}} R_{\text{in}}/\nu$
R_{in} = radius of inlet pipe or height at diffuser inlet
U_c = U_r at $\theta = 0$
U_{in} = average inlet velocity to diffuser
U_r = mean velocity along r direction
U_θ = mean velocity along θ direction
U_∞ = freestream velocity in planar diffuser
u_r = fluctuating velocity along r direction
u^+ = dimensionless U_r velocity, $= U_r/u_\tau$
u_θ = fluctuating velocity along θ direction
u_τ = wall friction velocity, $\sqrt{\tau_w/\rho}$
y_w = normal distance from diffuser wall
y^+ = dimensionless wall coordinate, $= y_w u_\tau/\nu$
$\delta_{0.99}$ = boundary-layer thickness measurement from the wall to $U_r = 0.99 U_\infty$
ϵ = dissipation rate of k
θ = circumferential coordinate
θ_0 = half divergence angle of diffuser
κ = von Kármán constant
μ = molecular viscosity of fluid
μ_t = turbulent viscosity
μ_{eff} = effective viscosity
ν = kinematic viscosity of fluid
ν_t = turbulent kinematic viscosity
$\sigma_k, \sigma_\epsilon$ = model constants

I. Introduction

DIFFUSERS are widely used to convert kinetic energy into pressure energy. The importance of the diffuser as a single, useful, fluid-mechanical element in wind tunnels and turbomachinery has been widely known. Therefore, the understanding of diffuser flows is of paramount importance to the design of turbomachines. A great deal of experimental and computational research have been devoted to this subject. Unfortunately, even turbulent flows in two-dimensional and conical diffusers are extremely complicated and our understanding of the details of energy transfer and dissipative losses inside a diffuser is still incomplete.

Vaneless (or radial) diffuser flows constitute the most complex type of flows because they are rotational, three-dimensional, and subject to an extremely high streamwise pressure gradient. Consequently, vaneless diffuser flows are difficult to investigate both experimentally and computationally. According to Bradshaw's[1] classification, whether a turbulent flow is "simple" or "complex" depends on the significant rate-of-strain component. In a simple shear flow, the important rate-of-strain is the gradient normal to the wall. On the other hand, a complex shear flow is one in which extra strain rates are present. It is known that even very small values of extra strain rates can have a significant effect on the turbulence field, thus invalidating the applicability of many turbulence models.[2] Since the various effects in a vaneless diffuser all lead to extra strain rates in the flow, the calculation of such flows requires

Received Dec. 2, 1987; revision received June 13, 1988; presented in part as Paper 88-3583 at the 1st National Fluid Dynamics Congress, Cincinnati, OH, July 25-28, 1988.

*Graduate Assistant, Mechanical and Aerospace Engineering.
†Professor, Mechanical and Aerospace Engineering.
‡Research Scientist.

increasingly more sophisticated turbulence models and is beyond the capability of current models.

Another feature of vaneless diffuser flow is its near-separation behavior, which is also common to other diffuser flows. Most turbulence models are inadequate for flows with high adverse pressure gradient effects. It is expected that a direct application of these models to vaneless diffuser calculations will not be appropriate. The least modification required of these models is a correction to account for high adverse pressure gradient effects. This modification can be easily validated by considering relatively simple diffusers, such as planar and conical diffusers. Therefore, the objectives of the present study are to develop such a model and to validate it in planar and conical diffuser flows.

As far as numerical predictions of turbulent planar and conical diffuser flows are concerned, most of the previous methods were based on boundary-layer approximations, and the solutions were obtained either by solving the integral equations[3,4] or by solving the modeled differential equations.[5] Since the boundary-layer solutions ignore the downstream effects on the upstream flow, the complicated pressure gradient effects in diffuser flows cannot be accounted for properly. Furthermore, the turbulence field near the diffuser wall is anisotropic and not in local equilibrium because of the presence of an adverse pressure gradient.[6] Therefore, accurate prediction of diffuser flows can be obtained only by solving elliptic governing equations that are closed with suitable turbulence models.

Recently, several elliptic methods were suggested. For example, Hah[7] proposed an elliptic method to calculate the properties of various turbulent flows in planar, conical, and annular diffusers. The turbulence closure was achieved by a conventional algebraic Reynolds stress model without correction for pressure gradient effects. Sindir[8] also made a calculation of the turbulent flow over a backward-facing step using algebraic Reynolds stress and k-ϵ closures. Since the above methods, including that used by Ilegbusi,[5] are based on the local equilibrium assumption and some kind of wall function to handle the near-wall flow, they are not suitable for diffuser flow calculations. In order to account for the anisotropic and nonequilibrium behavior near a wall, some kind of low Reynolds number turbulence model capable of resolving the flow all the way to the wall is preferred. As a first attempt, a low Reynolds number k-ϵ model suggested by Chien[9] is adopted because of its performance on simple turbulent shear flows. As expected, the model without modification cannot replicate the near-wall flow correctly, especially the prediction of the wall shear stress, in the presence of a severe adverse pressure gradient. It is conjectured that this could be the consequence of an inappropriate specification of the near-wall damping factor. A modification is proposed to Chien's model in order to properly account for pressure gradient effects. Therefore, the resultant model is capable of resolving near-wall turbulent flows subject to the action of a strong adverse pressure gradient. Recognizing the inadequacy of an isotropic model for near-separating and separating flows, a second objective of the program is to make use of the present results to modify a full Reynolds stress model for diffuser flow calculations. This effort will be the subject of a later report.

Although a lot of experimental work has been carried out on planar and conical diffusers,[10,11] few of them provide detailed measurements of nonseparating flow inside the diffuser, particularly in the near-wall region. Recently, Trupp et al.[6] made detailed measurements in the near-wall region of a nonseparating flow in a conical diffuser. The measurements are well documented and are most suitable for validating near-wall turbulence models with or without pressure gradient corrections. Furthermore, the experiments of Ref. 12 also provide reliable data for planar diffuser flows. Therefore, the measurements of Refs. 6 and 12 are chosen to validate the proposed low Reynolds number turbulence model and to demonstrate the inadequacy of the wall-function approximations and the necessity to correct for pressure gradient effects.

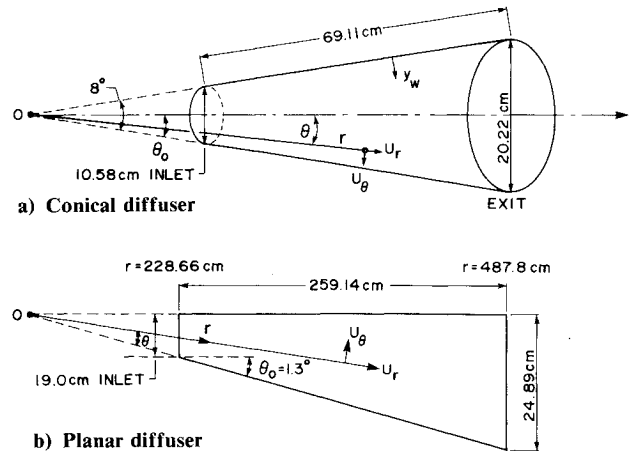

Fig. 1 Diffuser geometries and the coordinate systems used in the calculations.

II. Governing Equations and Turbulence Closure

The governing equations for an incompressible flow through a diffuser consist of continuity and conservation of linear momentum. If Reynolds decompositions are used to reduce these equations for turbulent flow analysis, unknown turbulent momentum flux terms appear in the resultant equations. These terms can be related to the known mean velocity field via suitable turbulence closures. Since the diffuser flow under consideration is very complex and greatly influenced by the severe adverse pressure gradient present in the diffuser, turbulence closures that rely on the wall-function approximations are not appropriate. A more suitable closure would be one that calculates the flow near the wall directly and thus be able to account for the viscous effects in the flow near a wall. Numerous near-wall flow models have been proposed. These include models based on the two-equation model of turbulence[9,13] and models based on the full Reynolds stress equations.[14,15] Even though these models are found to perform satisfactorily for a wide variety of complex turbulent flows,[16-18] their validity for flows with severe adverse pressure gradient effects has not been demonstrated. The necessity to modify the near-wall flow model to account for viscous and pressure gradient effects is amply demonstrated by the work of van Driest[19] and Cebeci et al.,[20] who proposed corrections to Prandtl's mixing length model for boundary-layer flows. In view of this, the low Reynolds number models should be modified to account for pressure gradient effects before application to diffuser flow calculations. As a first attempt, the present approach proposes to build on Chien's near-wall flow model.[9] Specifically, Chien's model is modified to take pressure gradient effects into account, so that the nonseparating, adverse pressure gradient flow in planar and conical diffusers can be calculated correctly.

The spherical coordinate system shown in Fig. 1a is used to describe the flow in the conical diffuser. For a stationary, incompressible, isothermal, and axisymmetric turbulent flow, the set of governing equations assuming the k-ϵ model of Chien[9] can be concisely written in spherical coordinates as

$$\frac{1}{r^2\sin\theta}\left[\frac{\partial}{\partial r}(\rho r^2 U_r \sin\theta) + \frac{\partial}{r\partial\theta}(\rho r^2 U_\theta \sin\theta)\right] = 0 \tag{1}$$

$$\frac{1}{r^2\sin\theta}\left[\frac{\partial}{\partial r}(\rho r^2 U_r\phi \sin\theta + \frac{\partial}{r\partial\theta}(\rho r^2 U_\theta\phi \sin\theta)\right]$$
$$= \frac{1}{r^2\sin\theta}\left[\frac{\partial}{\partial r}\left(r^2\sin\theta\frac{\mu_{\text{eff}}}{\sigma_\phi}\frac{\partial\phi}{\partial r}\right)\right.$$
$$\left. + \frac{\partial}{r\partial\theta}\left(r^2\sin\theta\frac{\mu_{\text{eff}}}{\sigma_\phi}\frac{\partial\phi}{r\partial\theta}\right)\right] + S_\phi \tag{2}$$

where ϕ represents U_r, U_θ, k, and ϵ, respectively, and the corresponding source terms are listed as

$$S_r = -\frac{\partial}{\partial r}\left(P + \frac{2}{3}\rho k\right) - \frac{4\mu_t + 2\mu}{r^2}U_r + \frac{1}{r^2}\frac{\partial}{\partial r}\left(r^2\mu_t\frac{\partial U_r}{\partial r}\right) + \frac{1}{r\sin\theta}\frac{\partial}{\partial\theta}\left[\sin\theta\cdot\mu_t\left(\frac{\partial U_\theta}{\partial r} - \frac{U_\theta}{r}\right)\right] - \frac{2\mu_{\text{eff}}}{r^2}\left(\frac{\partial U_\theta}{\partial\theta} + U_\theta\cot\theta\right) + \frac{\rho U_\theta^2}{r} \tag{3}$$

$$S_\theta = -\frac{\partial}{r\partial\theta}\left(P + \frac{2}{3}\rho k\right) - \left(\frac{\mu_t\cot^2\theta}{r^2} + \frac{\mu_{\text{eff}}}{r^2\sin^2\theta}\right)U_\theta - \frac{\rho U_r U_\theta}{r} + \frac{1}{r^2}\frac{\partial}{\partial r}\left[r^2\mu_t\left(\frac{\partial U_r}{r\partial\theta} - \frac{U_\theta}{r}\right)\right] + \frac{1}{r\sin\theta}\frac{\partial}{\partial\theta}\left[\sin\theta\cdot\mu_t\left(\frac{\partial U_\theta}{r\partial\theta} + \frac{2U_r}{r}\right)\right] + \frac{\mu_t + 2\mu}{r^2}\frac{\partial U_r}{\partial\theta} + \frac{\mu_t}{r}\frac{\partial U_\theta}{\partial r} - \frac{2\mu_t}{r^2}U_r\cot\theta \tag{4}$$

$$S_k = G - \rho\epsilon - \frac{2\mu k}{y_w^2} \tag{5}$$

$$S_\epsilon = C_{\epsilon 1}\frac{\epsilon}{k}G - C_{\epsilon 2}\rho f_1\frac{\epsilon^2}{k} - \frac{2\mu\epsilon}{y_w^2}\exp\left(\frac{-C_4 y_w\mu_\tau}{\nu}\right) \tag{6}$$

In the above equations, the Reynolds stresses are related to the mean-strain rate through the Boussinesq approximation. The turbulent viscosity μ_t is defined in terms of the turbulent kinetic energy and the dissipation rate as

$$\mu_t = \rho C_\mu f_\mu\frac{k^2}{\epsilon} \tag{7}$$

and the generation term G is given by

$$G = \mu_t\left[2\left(\frac{\partial U_r}{\partial r}\right)^2 + 2\left(\frac{1}{r}\frac{\partial U_\theta}{\partial\theta} + \frac{U_r}{r}\right)^2 + 2\left(\frac{U_r}{r} + \frac{U_\theta}{r}\cot\theta\right)^2 + \left(\frac{\partial U_\theta}{\partial r} + \frac{\partial U_r}{r\partial\theta} - \frac{U_\theta}{r}\right)^2\right] \tag{8}$$

Also, y_w is the distance measured from the wall. However, in the calculation, it is set equal to the product of the radial distance and the angle between the calculated point and the wall or $r(\theta_0 - \theta)$. This approximation is reasonable for diffusers with small divergence angle and the error introduced by this approximation is very small. The model functions and coefficients in the governing equations are given by Chien[9] as

$$f_\mu = 1 - \exp(-C_3 u_\tau y_w/\nu)$$

$$f_1 = 1 - (2/9)\exp[-(k^2/6\nu\epsilon)^2]$$

$$\sigma_{u_r} = 1.0,\quad \sigma_{u_\theta} = 1.0,\quad \sigma_k = 1.0,\quad \sigma_\epsilon = 1.3$$

$$C_{\epsilon 1} = 1.35,\quad C_{\epsilon 2} = 1.8,\quad C_\mu = 0.09,\quad C_4 = 0.5 \tag{9}$$

It should be noted that in Chien's model C_3 is a constant set equal to 0.0115. Since the model function f_μ is introduced in Eq. (7) to account for viscous damping effect near a wall as in van Driest's model,[19] any near-wall correction for pressure gradient effects should be incorporated into f_μ. One such suggestion has been proposed by Cebeci et al.[20] in their study of boundary-layer flows. In van Driest's[19] original proposal, the mixing length ℓ_m near a wall is given by

$$\ell_m = \kappa y(1 - e^{-cy^+}) \tag{10}$$

where $c = 0.038$ is assumed. Based on an analysis of the flow near a wall in the presence of a streamwise pressure gradient, Cebeci et al.[20] proposed a correction to Eq. (10). For the case of zero mass transfer, the modified expression is

$$\ell_m = \kappa y\{1 - \exp[-cy^+(1 - 11.8p^+)^{1/2}]\} \tag{11}$$

which predicts favorable pressure gradient flow rather well. Since μ_t near the diffuser wall can be expressed as $\mu_t = \ell_m^2(\partial U_r/r\partial\theta)$, the pressure gradient correction of Cebeci et al.[20] suggests that Eq. (7) can be similarly modified to account for streamwise pressure gradient effects. As a first attempt, a modification along the line of Eq. (11) is proposed for f_μ, such that

$$f_\mu = 1 - \exp[-C_3 y^+\text{ABS}(1 - C_5 p^+)] \tag{12}$$

This proposal asymptotes correctly to Chien's model when $p^+ \to 0$. On the other hand, the magnitude of the constant C_5 should be approximately equal to 11.8/2 if the linear version of Eq. (11) is taken for ℓ_m. This suggests that $C_5 \simeq 6.0$. However, later calculations of the conical diffuser flow shown in Fig. 1a reveal that $C_3 = 0.01113$ and $C_5 = 4.372$ give better agreement with the measurements of Trupp et al.[6] It should be pointed out that Eq. (12) is not intended for near-separating or separating flows because under those conditions p^+ will become very large and $(1 - C_5 p^+)$ becomes negative. Therefore, the range of p^+ in which Eq. (12) is applicable is determined, to a large extent, by the limiting value of f_μ, which should be taken as zero. However, Eq. (12) has no similar restrictions for favorable pressure gradient flows, because the limiting value of f_μ is one rather than zero.

The governing equations for the flow through a planar diffuser can be similarly derived. Here, instead of a spherical coordinate system, a cylindrical coordinate system is used. The diffuser half divergence angle is again denoted by θ_0. Since these equations can be easily written, they are not shown in order to avoid repetition.

III. Solution Technique

The discretization of the governing equations are obtained by integrating the differential equations over finite control volumes. Convection-diffusion formulation is based on a hybrid differencing scheme developed by Spalding.[21] The main hydrodynamic variables used in the computational scheme are velocities and pressure; the SIMPLE[22] algorithm is employed to solve the finite-difference equations for the velocity and pressure fields based on a staggered grid system. Each equation is solved by a line-by-line procedure using the tridiagonal matrix algorithm (TDMA). The solution procedure is as follows. A fixed pressure field is assumed and the momentum equations are solved. After each sweep over the solution domain, modifications are made to the pressure field to satisfy continuity. Transport equations for k and ϵ are then solved using the calculated velocity field. Iterations are carried out until the momentum and continuity equations are simultaneously satisfied. An accuracy criterion of relative mass and velocity residuals less than 0.1 percent is stipulated.

The calculations are performed to predict the experiments of Refs. 6 and 12. In Ref. 6, the measurements were obtained in a straight conical diffuser having a total divergence angle of 8 deg and an expansion ratio of 4:1. A fully developed pipe flow was established at the entrance to the diffuser. However, due to a lack of detailed measurements at the entry and also due to the geometric singularity at the juncture between the entrance straight pipe and the diffuser, the calculation starts at station 2, just downstream of the diffuser inlet. The solution domain and its dimensions are shown in Fig. 1a. Schraub and Kline's

experiments[12] were carried out to investigate the effects of pressure gradient on turbulent boundary layers; therefore, they included both favorable and adverse pressure gradient case, whose flow geometry is shown in Fig. 1b. This represents a planar diffuser flow with only one divergent wall. In order to avoid the geometric singularity right at the diffuser entrance, the calculation again starts at a location just downstream of the divergence. Nonuniform computational grids are used to resolve the flow in the region of interest. Based on the work of So and Yoo[15,17] and So et al.,[18] at least five grid points along the θ direction are prescribed between the wall and the grid point just outside of the viscous sublayer. Consequently, the low Reynolds number calculations are performed with 67 grid points specified in the θ direction. This is reduced to 46 points for the high Reynolds number closure where the wall-function approximations are assumed for the flow near the wall. As for the grid spacing in the streamwise or r direction, two different grid spacings are used: 51 and 91, respectively. Therefore, the flow through the planar and conical diffusers is carried out either with a grid of 51×67, 91×67, or 51×46.

Since p^+ is inversely proportional to u_τ^3, its value changes rapidly with u_τ. This will, in turn, cause f_μ to vary exponentially. Even though the actual flow does not approach separation, the computed flow could result in a very small u_τ at any one iteration step. The reasons for this are many; it could be due to incorrect guess of the pressure field or it could be due to an imbalance of momentum flux near the diffuser wall. When u_τ becomes very small or changes rapidly in any one iteration step, the numerical solution diverges. In order to prevent this from happening, one of two techniques can be implemented into the computational scheme. One procedure is to fix the exit p^+ value (either from the high Reynolds number results or from measurements) and adopts a curve-fitting technique for $u_\tau(r)$ at every iteration step. Another is to prescribe a $p^+(r)$ distribution based on the previously calculated u_τ, instead of evaluating $p^+(r)$ using the calculated $u_\tau(r)$ at each iteration step. These procedures prove to be quite successful in preventing a divergent solution from happening, even though they add to the overall computational time. The present calculations are carried out using the second procedure because it does not require p^+ to be fixed at the diffuser exit. With this implementation and a good initial guess for the pressure field in the conical diffuser, a convergent solution can be obtained after ~ 4000 iterations. The CPU time required is ~ 3600 s in an IBM 3090 mainframe computer. In general, the number of iterations and CPU time required for the planar diffuser calculation are about a factor of 2 less than those for the conical diffuser.

IV. Results and Discussion

Since Trupp et al.[6] offered detailed near-wall measurements of the flow in a conical diffuser, this data set is most suitable for validating the proposed turbulence model. In view of this, a careful comparison of the various model calculations with this data set is carried out first. The analysis also includes an examination of the effect of grid size on the calculated results to establish numerical credibility. This was carried out using the proposed turbulence model and two different grid sizes: one coarse (51×67) and one fine (91×67). Once the right grid size was identified, all other model calculations were carried out with the same grid. This way, the differences noted between various models are directly attributable to the modeling assumptions and are not a consequence of numerical errors. The same grid was also used to make the calculations of a planar diffuser flow, thus providing further validation for the proposed turbulence model. In the following, the conical diffuser flow is presented first, followed by a brief discussion of the planar diffuser flow.

Calculations of the conical diffuser flow of Trupp et al.[6] are carried out with the high Reynolds number k-ϵ model (designated H-k-ϵ), Chien's[9] model, and the modified low Reynolds number model discussed in Sec. II (designated L-k-ϵ). The boundary conditions for the diffuser flow are no slip at the wall for both the mean flow and turbulence quantities. At the inlet, $Re = 11.5 \times 10^4$ and U_r is obtained from the measurements of Ref. 6, whereas U_θ is taken to be zero. The turbulent kinetic energy is assumed to be the same as that of a fully developed pipe flow, whereas the dissipation rate of k at the inlet is approximated by

$$\epsilon = \frac{k^{3/2}}{0.2R_{\text{in}}} \tag{13}$$

based on the equilibrium assumption and the data of Laufer.[23] At the centerline, the θ derivatives of all flow quantities are assumed to be zero, while at the exit the second r derivatives of the flow variables are set equal to zero.

The conical diffuser flow experiment of Trupp et al.[6] indicates that the turbulent flow in a conical diffuser generally can be divided into three major flow regimes. One regime is near the diffuser centerline and is the inviscid core region where the influence of the wall is essentially negligible. Another is the near-wall flow region, which is similar to the near-wall flow of a turbulent boundary layer subject to severe adverse pressure gradient effects. Due to the presence of the severe adverse pressure gradient, the turbulence structure is not in local equilibrium and the log-law slope is greatly affected. The region between these two represents a highly distorted turbulent flow with the turbulence levels and rates of turbulence production and dissipation greatly in excess of their corresponding values in a zero-pressure-gradient boundary layer.[24] Measurements by Trupp et al.[6] seem to suggest that this region is like some kind of "outer" boundary layer representing the decaying remnant of the inlet turbulent pipe flow.

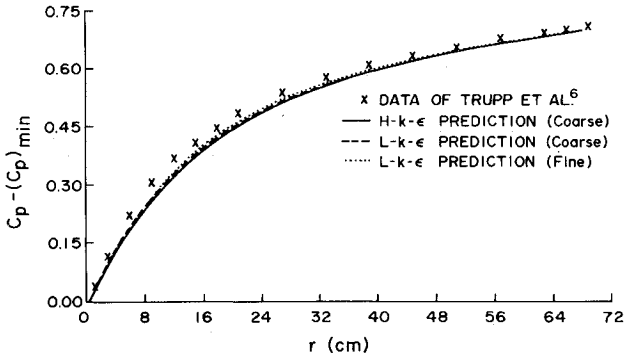

Fig. 2 Comparison of calculated and measured pressure coefficient for the conical diffuser.

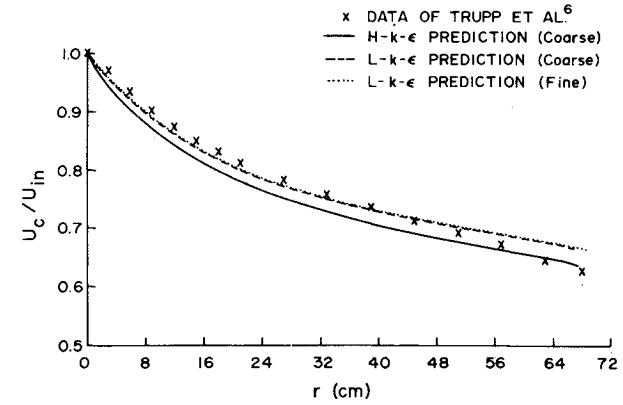

Fig. 3 Comparison of calculated and measured centerline velocity U_c for the conical diffuser.

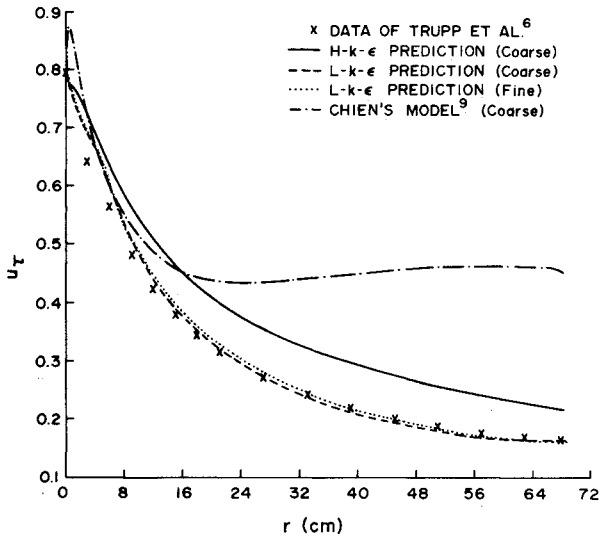

Fig. 4 Comparison of calculated and measured wall friction velocity u_τ for the conical diffuser.

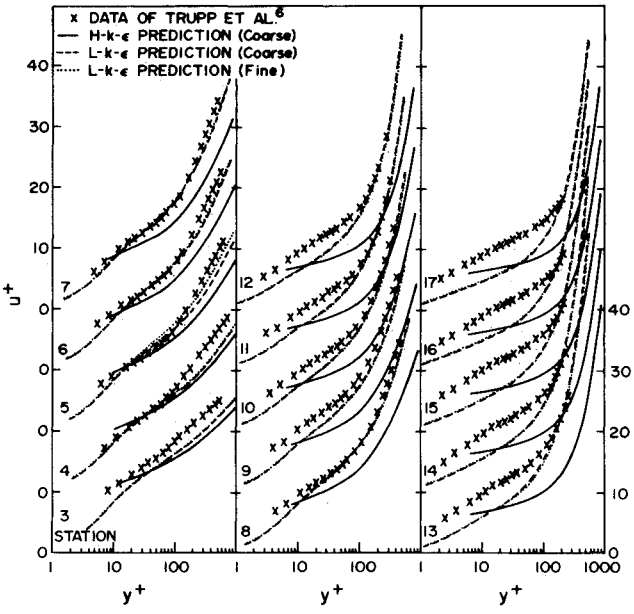

Fig. 5 Comparison of calculated and measured near-wall velocities in universal coordinates for the conical diffuser.

Since the flow in the inviscid core region is not greatly affected by the near-wall flow, the prediction of the flow behavior in this region should be quite independent of the turbulence model used. Furthermore, the pressure increase in a diffuser with a nonseparating flow is primarily determined by the expansion ratio and is not much influenced by the viscous loss near the wall. This again suggests that the pressure coefficient in a conical diffuser can be correctly calculated independent of the near-wall turbulence model invoked. These arguments are essentially substantiated by the comparison of the pressure coefficient and the centerline velocity distribution shown in Figs. 2 and 3. The agreement between the two model calculations and measurements of $C_p - (C_p)_{\min}$ is excellent (Fig. 2), which suggests that, for nonseparating flow in a conical diffuser, the pressure rise is basically an inviscid phenomenon. As for the centerline velocity distribution, a slight discrepancy is noted between the measurements and the H-k-ϵ model results. On the other hand, the L-k-ϵ model result is in good agreement with measurements. This suggests that, to a limited extent, the inviscid core region is influenced by the near-wall flow. In both Figs. 2 and 3, the fine-grid results obtained from the L-k-ϵ model are also shown. They are identical to the coarse-grid results. This shows that the coarse-grid results are essentially grid independent. Since the diffuser core flow is not affected by near-wall turbulence models, Chien's model results for U_c and $C_p - (C_p)_{\min}$ are also found to be identical to those shown in Figs. 2 and 3. Therefore, they are not plotted in the figures.

The measurements of Trupp et al.[6] are carried out in the near-wall region, and no measurements are available in the middle region. Furthermore, turbulence measurements are not made at all. However, detailed near-wall flow measurements down to $y^+ = 4$ are available. Therefore, this particular data set is most suitable for the validation of near-wall flow models. In view of this, the following comparisons are carried out with the near-wall flow data alone. A comparison of the outer region will have to wait until more data are available.

A comparison of the calculated and measured u_τ is shown in Fig. 4. This figure also shows the results of Chien's model. It can be seen that Chien's model greatly overpredicts u_τ in the region very near the inlet and also in the region downstream of $r = 10$ cm. Instead of predicting a continuous decrease in u_τ, Chien's model gives a slight u_τ increase after $r \simeq 24$ cm. The increase continues toward the diffuser exit. On the other hand, the H-k-ϵ model result is correct qualitatively but quantitatively higher than the measurements all along the diffuser. Therefore, these calculations clearly indicate that Chien's model and the wall-function approximations are not valid for nonseparating conical diffuser flow. The L-k-ϵ model result, on the other hand, is in excellent agreement with the data, except for a short region near the diffuser inlet. This discrepancy could be due to an incorrect specification of the flow at the inlet. In this calculation, fully developed pipe flow turbulence is assumed at the diffuser inlet, which may not be correct. However, this inlet effect only extends to ~ 5 cm downstream. Thereafter, the calculated flow is not affected by the inlet condition at all. This suggests that the L-k-ϵ model is not too sensitive to the inlet condition specified.

Further evidence that the L-k-ϵ model is far superior than the H-k-ϵ model is provided by a comparison of the near-wall velocity profiles. Chien's model results are not compared in the following because of the grossly inaccurate u_τ that renders the near-wall flow comparison invalid. However, the fine-grid results also are shown to demonstrate the grid-independent character of the coarse-grid results. According to Trupp et al.,[6] the near-wall velocity profile can be described by a log region, a half-power region, and a linear region. Typically, the half-power region represents the transition from the near-wall ($y^+ < 40$) log region to the outer ($y^+ > 70$) linear region. The exact locations of y^+ where the log behavior changes to half-power behavior and finally to linear behavior, of course, depend on the r position along the diffuser. Furthermore, the data also show that the von Kármán constant κ varies from 0.41 to a minimum of 0.3 before slowly increasing back to 0.38 as the pressure gradient increase begins to slow down in the diffuser. All these features are correctly predicted by the L-k-ϵ model. A comparison of the log behavior between model calculations and measurements is shown in Fig. 5, while the corresponding comparisons of the half-power and linear behavior are given in Figs. 6 and 7, respectively. The H-k-ϵ model and fine-grid results are also compared in Fig. 5, but they are not shown in Figs. 6 and 7. It is obvious from the comparison shown in Fig. 5 that the H-k-ϵ model is totally inadequate in the calculation of nonseparating flow in conical diffusers. Inherent in the wall function approximations is a constant κ. This, of course, is not true in an adverse pressure gradient flow. On the other hand, the coarse and fine grid L-k-ϵ model results reproduce correctly the behavior of κ in the presence of adverse pressure gradient effects. This is clearly illustrated in Fig. 5, where the calculated slopes of the velocity profiles in the log region are in good agreement with the measured slopes.

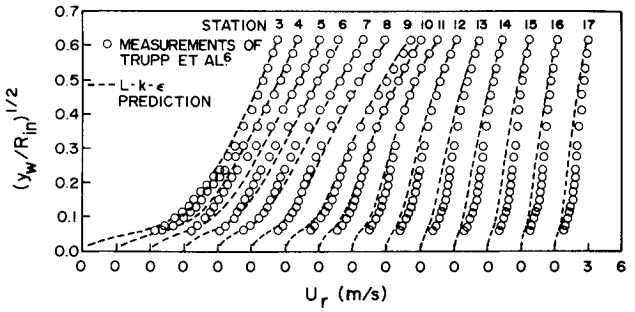

Fig. 6 Comparison of calculated and measured near-wall velocities in half-power coordinate for the conical diffuser.

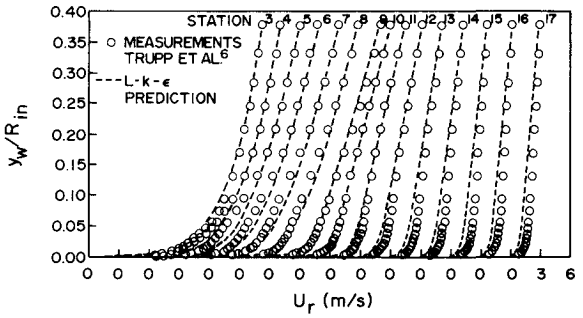

Fig. 7 Comparison of calculated and measured near-wall velocity distributions in linear coordinate for the conical diffuser.

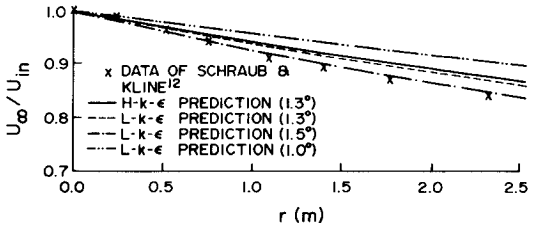

Fig. 8 Comparison of calculated and measured U_∞ for the planar diffuser.

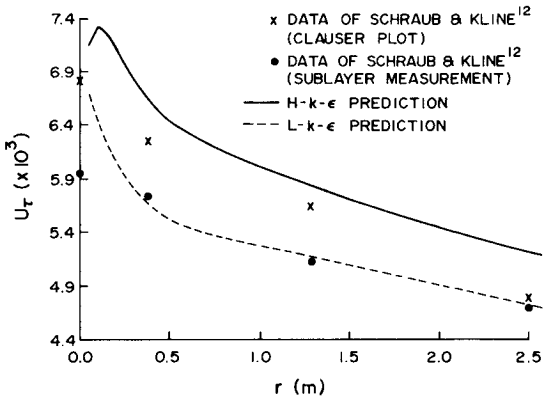

Fig. 9 Comparison of calculated and measured u_τ for the planar diffuser.

It should be pointed out that discrepancies do exist between the L-k-ϵ model calculations and measurements (Fig. 5), especially approaching the diffuser exit. There are several reasons for the discrepancies. The first is the isotropic turbulence assumption of the L-k-ϵ model. However, the experimental results of Okwuobi and Azad[25] show strong anisotropy in a conical diffuser flow. In order to remedy this situation, it is suggested that the full Reynolds stress model of So and Yoo[15] should be modified to account for pressure gradient effects. A second reason is the exit boundary condition imposed on the calculations. Lacking a better condition, the second r derivatives of all flow quantities are set equal to zero in the present calculations, but the measurements do not seem to provide strong support for this assumption. Finally, the pressure gradient correction proposed in Eq. (12) may not be the most suitable. However, in view of the excellent agreement shown in u_τ, Eq. (12) seems to be able to replicate the wall friction behavior correctly.

A second validation of the proposed L-k-ϵ model is provided by the measurements of Ref. 12. Since Chien's model has been shown to be inappropriate for flows with adverse pressure gradient effects, it is not used to calculate the planar diffuser flow. Also, in the conical diffuser flow calculations, it is established that a 51×67 grid or a 51×46 grid is sufficient to give grid-independent results, depending on the turbulence model used. Therefore, in calculating the planar diffuser flow, only coarse grids are specified. Consequently, the planar diffuser flow measurements are compared with the L-k-ϵ and H-k-ϵ model results obtained from the coarse grids only. The boundary conditions are no slip at the walls for both the mean flow and turbulence quantities. At the inlet, measured profiles of U_r is specified. The k and ϵ distributions within the boundary layers of the inlet flow are approximated by universal flat-plate boundary-layer values.[24] Outside the wall boundary layers, the flow is considered to be uniform and free of turbulence. The inlet Re is 6.75×10^4. At the exit, the second r derivatives of the flow quantities are a gain set equal to zero.

In the report, Schraub and Kline[12] specified the diffuser divergence angle as 1 deg. However, the calculated divergence angle based on the specified diffuser geometry is 1.3 deg. The report also provided measurements of U_∞, the stream velocity outside the boundary layer on the nondivergent flat wall (Fig. 1b). If the calculated U_∞ from the L-k-ϵ model was to agree with the measured U_∞, then a divergence angle of 1.5 deg has to be assumed (Fig. 8). The calculated u_∞ distributions assuming a divergence of 1 and 1.3 deg also are shown in Fig. 8 for comparison. It can be seen that the 1 deg divergence calculation is substantially different from the measurements. Since the 1.5 deg divergence is not consistent with the specified diffuser geometry, the calculation of the planar diffuser flow is carried out on the geometry shown in Fig. 1b with a divergence of 1.3 deg on one of the walls. The H-k-ϵ model calculation assuming a divergence of 1.3 deg is also shown in Fig. 8. As expected, there is only a slight difference between the H-k-ϵ and L-k-ϵ results, which essentialy substantiates the conclusion drawn from the conical diffuser calculation.

The u_τ comparison is shown in Fig. 9. Schraub and Kline[12] reported two measurements of u_τ, one based on Clauser plot of the measured velocity profiles and another on near-wall measurements of the velocity. All their measurements were obtained from the nondivergent flat wall. The near-wall measurements consistently give a u_τ that is quite a bit lower than the u_τ determined from the Clauser plots. Based on measurements by Trupp et al.,[6] the log-law slope changes as the flow moves through the diffuser. Since the Clauser plot is based on the existence of a log-law region with a constant slope, its application to determine u_τ in any diffuser flow is not appropriate. Therefore, the various Clauser-plot u_τ reported by Schraub and Kline[12] are not reliable. The u_τ calculated from the L-k-ϵ model are in excellent agreement with those determined from near-wall measurements of U_r, but they are substantially lower than those obtained from Clauser plots. As expected, the H-k-ϵ results are greater than both sets of u_τ reported in Ref. 12. For the reasons stated above, it is believed that the u_τ derived from the near-wall measurements are more reliable. Therefore, once again, the L-k-ϵ model predicts the diffuser flow correctly.

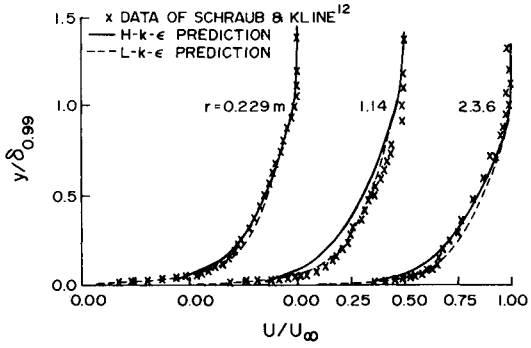

Fig. 10 Comparison of calculated and measured velocity profiles for the planar diffuser.

Finally, a comparison of the calculated and measured velocity profiles is shown in Fig. 10. The result again bears out the conclusion drawn from the conical diffuser calculation, namely, that the L-k-ϵ model is most suitable for diffuser flow calculations and the H-k-ϵ model is not valid for flows with adverse pressure gradient effects.

V. Conclusions

The following major conclusions emerge from this study:

1) The high Reynolds number k-ϵ model with its associated wall-function approximations is not applicable to planar and conical diffuser flow calculations, even though it is able to predict the behavior of the pressure coefficient and centerline velocity correctly.

2) The low Reynolds number k-ϵ model of Chien[9] without pressure gradient correction also is not applicable to planar and conical diffuser flow calculations because it leads to gross momentum imbalance near the wall.

3) The L-k-ϵ model reproduces the near-wall turbulent flow in planar and conical diffusers quite well, but some discrepancy exists between the calculated and measured mean velocity profiles at very high adverse pressure gradient.

4) The underlying assumption of isotropic turbulence seems to be a major drawback of the L-k-ϵ model. Better results could be obtained through the use of more sophisticated models, such as Reynolds stress closures that allow for anisotropic behavior of turbulence near a wall. Therefore, our next logical step is to extend the Reynolds stress model to calculate diffuser flows and to provide a more complete comparison of the flow properties.

Acknowledgment

The first two authors wish to acknowledge support given them by the David Taylor Naval Ship Research and Development Center, Annapolis, MD, under Contract N00167-86-K-0075.

References

[1]Kline, S. J., Cantwell, B., and Lilley, G. M. (eds.), *Complex Turbulent Flows: Comparison of Computation and Experiment,* Vol. II, Stanford University Press, Stanford, CA, 1982.

[2]Lakshminarayana, B., "Turbulence Modeling for Complex Shear Flows," *AIAA Journal,* Vol. 24, Dec. 1986, pp. 1900–1917.

[3]Bardina, J., Lyrio, A., Kline, S. J., Ferziger, J. H., and Johnston, J. P., "A Prediction Method for Planar Diffuser Flows," *Journal of Fluids Engineering,* Vol. 103, June 1981, pp. 315–321.

[4]Strawn, R. C., Ferziger, J. H., and Kline, S. J., "A New Technique for Computing Viscous-Inviscid Interactions in Internal Flows," *Journal of Fluids Engineering,* Vol. 106, March 1984, pp. 79–84.

[5]Illegbusi, J. O., "Numerical Calculation of Steady Turbulent Flows in Adverse Pressure Gradients," *Engineering Analysis,* Vol. 1, No. 2, 1984, pp. 70–77.

[6]Trupp, A. C., Azad R. S., and Kassab, S. Z., "Near-Wall Velocity Distributions within a Straight Conical Diffuser," *Experiments in Fluids,* Vol. 4, No. 8, 1986, pp. 319–331.

[7]Hah, C., "Calculation of Various Diffuser Flows with Inlet Swirl and Inlet Distortion Effects," *AIAA Journal,* Vol. 21, 1983, pp. 1127–1133.

[8]Sindir, M. M. S., "A Numerical Study of Turbulent Flows in Backward-Facing-Step Geometries: A Comparison of Four Models of Turbulence," Ph.D. Dissertation, University of California, Davis, 1982.

[9]Chien, K. Y., "Predictions of Channel and Boundary Layer Flows with a Low-Reynolds-Number Turbulence Model," *AIAA Journal,* Vol. 20, No. 1, 1982, pp. 33-38.

[10]Ashjaee, J., Johnston, J. P., and Kline, S. J., "Subsonic Turbulent Flow in Planar-Wall Diffusers: Peak Pressure Recovery and Transitory Stall," Thermoscience Div, Dept. of Mechanical Engineering, Stanford University, Stanford, CA, Rept. PD-21, 1980.

[11]Pozzorini, R., "Das Turbulente Stromugsfeld in Einem Langen Kreiskegel-Diffusor," Ph.D. Dissertation 5646, Eidgenossischen Technischen Hochschule, Zurich, 1976.

[12]Schraub, F. A. and Kline, S. J., "A Study of the Structure of the Turbulent Boundary Layers with and without Longitudinal Pressure Gradients," Thermosciences Div., Stanford University, Stanford, CA, Rept. MD-12, 1965.

[13]Jones, W. P. and Launder, B. E., "The Prediction of Laminarization with a Two-Equation Model of Turbulence," *International Journal of Heat and Mass Transfer,* Vol. 15, No. 2, 1972, pp. 301–314.

[14]Kebede, W., Launder, B. E., and Younis, B. A., "Large Amplitude Periodic Pipe Flow: A Second Moment Closure Study," *Proceedings of 5th Turbulent Shear Flows Symposium*, Ithaca, NY, 1985, p. 16.23-16.29.

[15]So, R. M. C. and Yoo, G. J., "On the Modelling of Low Reynolds Number Turbulence," NASA CR-3994, July 1986.

[16]Patel, V. C., Rodi, W., and Scheuerer, G., "Turbulence Models for Near-Wall and Low Reynolds Number Flows: A Review," *AIAA Journal*, Vol. 23, Sept. 1985, pp. 1308–1319.

[17]So, R. M. C. and Yoo, G. J., "Low-Reynolds-Number Modelling of Turbulent Flows with and without Wall Transportation," *AIAA Journal*, Vol. 25, Dec. 1987, pp. 1556–1564.

[18]So, R. M. C., Lai, Y. G., Hwang, B. C., and Yoo, G. J., "Low-Reynolds-Number modelling of Flows over a Backward-Facing-Step," *Zeitshrift für angewandte Mathematik und Physik*, Vol. 39, No. 1, 1988, pp. 13–27.

[19]van Driest, E. R., "On Turbulent Flow Near a Wall," *Journal of the Aeronautical Sciences*, Vol. 23, 1956, pp. 1007–1011.

[20]Cebeci, T., Smith, A. M. O., and Mosinskis, G., "Solution of the Incompressible Turbulent Boundary Layer Equations with Heat Transfer," *Journal of Heat Transfer*, Vol. 92, 1970, pp. 133–143.

[21]Spalding, D. B., "A Novel Finite-Difference Formulation for Differential Expressions Involving Both First and Second Derivatives," *International Journal of Numerical Methods in Engineering*, Vol. 4, 1972, pp. 551–559.

[22]Patankar, S. V. and Spalding, D. B., "A Calculation Procedure for Heat, Mass and Momentum Transfer in Three-Dimensional Parabolic Flows," *International Journal of Heat and Mass Transfer*, Vol. 15, 1972, pp. 1787–1806.

[23]Laufer, J., "The Structure of Turbulence of Fully Developed Pipe Flow," NACA Rept. 1174, 1954.

[24]Klebanoff, P. S., "Characteristics of a Boundary Layer with Zero Pressure Gradient," NACA TN-3178, 1954.

[25]Okwuobi, P. A. C. and Azad, R. S., "Turbulence in a Conical Diffuser with Fully-Developed Flow at Entry," *Journal of Fluid Mechanics*, Vol. 57, No. 3, 1973, pp. 603–622.